Effect of dephasing on mesoscopic conductance fluctuations in quantum dots with single channel leads

Edward McCann[1] and Igor V. Lerner[2,3]
[1] *Max-Planck-Institut für Physik komplexer Systeme, Nöthnitzer Str. 38, 01187 Dresden, Germany*
[2] *School of Physics and Space Research, University of Birmingham, Birmingham B15 2TT, United Kingdom*
[3] *Isaac Newton Institute for Mathematical Sciences, Cambridge CB3 0EH, United Kingdom*
(February 1, 2008)

We consider the distribution of conductance fluctuations in disordered quantum dots with single channel leads. Using a perturbative diagrammatic approach, valid for continuous level spectra, we describe dephasing due to processes within the dot by considering two different contributions to the level broadening, thus satisfying particle number conservation. Instead of a completely non-Gaussian distribution, which occurs for zero dephasing, we find for strong dephasing that the distribution is mainly Gaussian with non-universal variance and non-Gaussian tails.

PACS numbers: 73.23.-b, 72.15.-v, 73.20.Fz, 85.30.Vw

I. INTRODUCTION

Soon after the theoretical prediction of universal conductance fluctuations (UCF) in disordered electronic samples,[1–4] it was shown that their distribution function is mainly Gaussian.[5] These considerations referred to a weakly disordered *open* sample connected to a reservoir by broad external contacts. In this case, after diffusing through the sample of size L during time $\tau_{\rm erg} \sim L^2/D$ electrons are inelastically scattered in the reservoir (D is the diffusion coefficient). The resulting uncertainty in the level position, i.e. level broadening γ, is of the order of the Thouless energy $E_c = \hbar/\tau_{\rm erg}$, and $E_c \gg \Delta$, where Δ is the mean level spacing. This picture remains almost unchanged in the presence of relatively strong inelastic processes within the sample[3,4] which lead to dephasing (the loss of phase-coherence) at the time scale $\tau_\phi \lesssim \tau_{\rm erg}$: the conductance distribution remains almost Gaussian although its variance is no longer universal but decreases $\propto (\tau_\phi/\tau_{\rm erg})^{2-d/2}$ where d is a spatial dimensionality.

In contrast, it has been shown more recently that the conductance distribution is pronouncedly non-Gaussian in almost closed systems like chaotic cavities with single channel leads[6,7], quantum dots in the regime of Coulomb blockade[8,9] where the distribution of the heights of the Coulomb blockade peaks has been measured experimentally,[10] or isolated conducting rings threaded by an Aharonov–Bohm flux.[11] Weak transmission through the contacts means that the electrons typically spend more time in the system than $\tau_{\rm erg}$ so the broadening of energy levels $\gamma \ll E_c$. This inequality corresponds to the ergodic regime which allows the use of non-perturbative techniques including random matrix theory[12,13] and the zero dimensional supersymmetric σ model.[14]

There are two distinct types of behavior within the ergodic regime, depending on whether the level broadening γ is smaller or larger than the mean level spacing Δ. In the absence of level overlapping, $\gamma \ll \Delta$, the conductance distribution is clearly non-Gaussian. The nature of the distribution changes considerably when dephasing is substantial, $\gamma \gtrsim \Delta$, so that the energy levels overlap. This case allows also a perturbative treatment[15] in the framework of the standard diagrammatic expansion. A crucial question here is how to describe the level broadening in quantum dots with point-like external contacts. The first approach, following Ref. 16, was to attach an additional voltage probe in which electrons lose their phase coherence before being re-injected into the dot.[17] Another approach was to include an imaginary potential in the Hamiltonian thus allowing for the possibility that electrons may leave the dot.[7,9,15] However, Brouwer and Beenakker[18] have recently pointed out that these approaches do not describe inelastic processes *within* the dot. While the voltage probe accounts for spatially localized dephasing only, the imaginary potential in the Hamiltonian does not conserve the particle number. In order to describe dephasing processes within the dot, they have introduced[18] in the framework of random matrix theory a new variant of the voltage probe model which produces spatially uniform dephasing. Thus it was found that the conductance distribution became Gaussian for strong dephasing, $\tau_\phi \ll \hbar/\Delta$. Note that experiments measuring conductance fluctuations in quantum dots, for example as a function of shape,[19] also find a Gaussian distribution.

In this paper we present a microscopic diagrammatic calculation of the conductance distribution function within a dirty quantum dot with two point contacts in the presence of strong dephasing processes ($\tau_\phi \ll \hbar/\Delta$) within the dot. We construct a particle-conserving model by clearly separating two different mechanisms of level broadening: dephasing processes which contribute only to the conductance fluctuations and particle leakage which contributes also to the mean value of conductance. It enables us to resolve a contradiction between the results of the imaginary potential model[7,9,15] that suffered from the violation of particle conservation

and the voltage-probe model.[17,18] By calculating the moments of the conductance distribution, we will show that for $\tau_\phi \ll \hbar/\Delta$ it is almost Gaussian with the variance

$$\operatorname{var} G = \frac{4\zeta_\phi(\ell)}{\beta}\,\langle G\rangle^2\,. \tag{1}$$

This expression is valid both in the ergodic zero-mode regime, $\tau_\phi \gg \tau_{\rm erg}$, and in the diffusive regime, $\tau_\phi \ll \tau_{\rm erg}$. Here $\langle G\rangle$ is the mean conductance, and $\zeta_\phi(\ell) \equiv \zeta_\phi(R{=}\ell)$ where the small parameter $\zeta_\phi(R)$ is effectively a diffusion propagator at distance R in the presence of strong dephasing, and ℓ is the elastic mean free path. We will show that this parameter is given by

$$\zeta_\phi(R) \approx \begin{cases} g_0^{-1}\ln(L_\phi/R), & \tau_\phi \ll \tau_{\rm erg}, \quad d=2 \\ (\pi/2g_0)\,(\ell/R), & \tau_\phi \ll \tau_{\rm erg}, \quad d=3 \\ \Delta\tau_\phi/\pi, & \tau_\phi \gg \tau_{\rm erg}, \quad \text{any } d \end{cases} \tag{2}$$

Here $L_\phi = (D\tau_\phi)^{1/2}$ is the dephasing length. Note that although the voltage-probe model[18] also predicts a Gaussian conductance distribution, the width of the distribution given by Eq. (1) is different from that obtained in Ref. 18. In contrast to a cavity with broad leads,[20] (which corresponds to a multi-channel case so that the fluctuations remain universal) the variance is non-universal even in the diffusive regime, $\tau_\phi \ll \tau_{\rm erg}$.

The factor $\zeta_\phi(\ell)$ which governs the distribution width resembles the standard weak-localization parameter. This could be seen from the first line of Eq. (2) where $g_0 \sim E_c/\Delta$ is a classical dimensionless conductance of a sample with broad leads. Nevertheless, the origin of this parameter is quite different: the variance is not very sensitive to the presence of a magnetic field and thus has nothing to do with weak localization effects. When time-reversal invariance is absent, the variance (1) changes only by the standard Dyson's factor of $1/\beta$, typically for mesoscopic effects, where $\beta = 1$ for the orthogonal ensemble (in the presence of potential scattering only), and $\beta = 2$ for the unitary ensemble (in the presence of a finite magnetic field or weak scattering by magnetic impurities that breaks time-reversal symmetry).

It is worth noting that the close-to-Gaussian nature of the distribution is established in a way somewhat less straightforward than for UCF in samples with broad leads.[5] Had it been possible to restrict considerations to the lowest order of perturbation for the variance and higher moments, we would have obtained the exponential distribution as in the imaginary potential model,[7,9,15] albeit with a shifted position of the mean. However, the leading contribution to the moments is given by the next (two-loop) order of perturbation while contributions from higher orders are negligible.

II. TWO KINDS OF DIFFUSONS

In considerations of conductance fluctuations in quantum dots with single-channel leads, the lowest order of perturbation does not make a leading contribution due to the existence of two different perturbative parameters related to qualitatively different contributions to the level broadening. Although both of them arise also in considering any mesoscopic effect for a diffusive sample with broad contacts, only one of them is relevant in that case as we explain below.

We adopt the impurity diagram technique[21] to perform ensemble averaging over disorder with allowance for dephasing processes. At the first step, we assume a conventional model of free electrons in a random Gaussian potential V, with $\langle V(r)\rangle = 0$ and

$$\langle V(\boldsymbol{r})\,V(\boldsymbol{r'})\rangle = \frac{1}{2\pi\nu_0\tau_{\rm el}}\,\delta(\boldsymbol{r}-\boldsymbol{r'})\,, \tag{3}$$

where ν_0 is the one-electron density of states and $\tau_{\rm el}$ is the mean elastic scattering time. A standard perturbative expansion[22] is a loop-expansion with the loops being built up of diffusons and Cooperons (if time reversal symmetry is preserved). These are impurity ladders (Fig. 1) with a pole at small transferred momenta (diffusons) or small total momenta (Cooperons). For an isolated d-cubic sample of size L with $L \gg \ell$ such a diffusion propagator (*diffuson*) at $T = 0$, i.e. in the absence of inelastic processes, is given by

$$\mathcal{D}(\mathbf{q};\omega) = \frac{1}{2\pi\nu_0\tau_{\rm el}^2}\,\frac{1}{D\boldsymbol{q}^2 - i\omega}\,, \tag{4}$$

where $D = v_F^2\tau_{\rm el}/d$ is the diffusion constant, $v_F\tau_{\rm el} = \ell$, and $\boldsymbol{q} = \pi\boldsymbol{n}/L$ with $\boldsymbol{n} = (n_1,\ldots,n_d)$ being non-negative integers. In the presence of time reversal symmetry, the Cooperon propagator has the same form.

For weak disorder, the diffusion propagator is proportional to the Fourier transform of the density-density correlation function,

$$K(\mathbf{r};t) \equiv \langle\,\rho(0,0)\,\rho(\boldsymbol{r},t)\,\rangle\,, \tag{5}$$

which describes the probability of finding at the point $\boldsymbol{r}$ at time t a diffusive particle injected at the origin at $t = 0$. Particle conservation implies that $\int K(\mathbf{r};t)d^dr = \text{const}$ at any time $t \geq 0$. On performing the Fourier transform, one then obtains that $\mathcal{D}(0;\omega) = \text{const}/\omega$.

This exact identity remains valid also at $T \neq 0$ when one includes a weak interaction leading to dephasing processes in the sample. Therefore, the diffuson associated with $K(\mathbf{r};t)$ remains the same as in Eq. (4): the only possible effect of dephasing could be in replacing D with $D_{\rm eff}$ (for weak disorder, $|D_{\rm eff} - D| \ll D$ so that this effect may also be neglected).

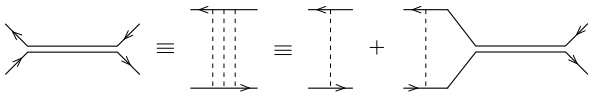

FIG. 1. A diffuson ladder. A Cooperon ladder is obtained by inverting the direction of one of the arrows.

Mathematically, particle conservation in the diffuson associated with the density-density correlation function (which we call *the intrinsic diffuson*) is due to the Ward identity which provides an exact cancellation of the one-particle self-energy corrections due to inelastic processes by vertex corrections (described graphically as interaction lines between the two sides of the diffusion ladders). However, if one defines the diffuson in terms of the sum of graphs describing diffusive propagation in the particle-hole channel *without energy exchange* between the particle and hole line, it is no longer proportional to the density-density correlation function and it is not constrained by particle conservation.[23] The absence of the usual cancellation of self-energy corrections by vertex corrections leads to the appearance of the cutoff τ_ϕ^{-1} in the diffusion pole.[4,23] This is precisely the kind of diffuson arising in typical lowest-order conductance-fluctuations diagrams[1–5] and describing correlations between *different members of the ensemble* which makes energy exchange between the opposite sides of the diffusion ladder impossible. We will call this kind of diffuson *inter-sample*. Note that all the Cooperon propagators, either intrinsic or inter-sample, have exactly the same cutoff, τ_ϕ^{-1}, as the inter-sample diffusons.[4]

Therefore, one can allow for dephasing by merely including τ_ϕ^{-1} as an infrared cutoff in the denominators of *inter-sample* diffusons, i.e. substituting into Eq. (4) τ_ϕ^{-1} for $-i\omega$ at zero frequency. At $T \neq 0$, averaging over energies leads[3,4] to the saturation of the denominators of *inter-sample* diffusons. A consistent description of both thermal smearing and dephasing requires the use of the temperature technique[21] and the development of a microscopic theory of dephasing in the partially open dot which would provide a dependence of τ_ϕ on T and microscopic characteristics of the dot. Such a theory is well established for relatively large diffusive samples with broad leads[24] or for closed quantum dots.[25]

However, our aim here is just to describe how dephasing and thermal smearing influence mesoscopic fluctuations of conductances of the dot. To this end, all we need is to distinguish between the two kinds of diffusons: *inter-sample* diffusons which are saturated at $q = \omega = 0$, and *intrinsic* diffusons which diverge at $q = \omega = 0$. Since the divergence of this sort could not be treated within the diagrammatic approach, we introduce a weak level broadening $\gamma_{\rm esc}$ due to escape from the dot which provides a cutoff for the *intrinsic* diffusons. The cutoff in the intrinsic diffuson violates the particle conservation law but since we restrict our considerations to the case $\gamma_{\rm esc} \ll \min(T, \hbar/\tau_\phi)$, it is dephasing (or thermal smearing) within the dot rather than particle escape which governs the conductance distribution. Even with this cutoff, $\mathcal{D}_\phi(q = \omega = 0) \ll \mathcal{D}_{\rm esc}(q = \omega = 0)$, i.e. there is a sharp distinction between the *intrinsic* diffusons, $\mathcal{D}_{\rm esc}$, and the *inter-sample* diffusons, $\mathcal{D}_\phi$. For simplicity, we shall use a zero-temperature diagrammatic technique. If $T > \hbar/\tau_\phi$, one should substitute T for $\hbar/\tau_\phi$ and the thermal-smearing length $L_T = (\hbar D/T)^{1/2}$ for the dephasing length L_ϕ in all final results, including that for the variance, Eq. (1).

The existence of the two kinds of diffusons was practically irrelevant for the description of mesoscopic conductance fluctuations in samples with broad leads.[1–5] Firstly, there is strong leakage through the leads, $\gamma \sim \hbar/\tau_{\rm erg}$, and one could restrict considerations to the case of weak dephasing, $\tau_{\rm erg} \ll \tau_\phi$, when both intrinsic and inter-sample diffusons have the same cutoff. Moreover, even for larger samples or higher temperatures when $\tau_{\rm erg} \gg \tau_\phi$, the intrinsic diffusons do not appear either in $\langle G\rangle$ or in var$G$ but as a third-order perturbation correction which is irrelevant in a weakly disordered metal. In contrast to this, in the problem under consideration the intrinsic diffusons determine the value of $\langle G\rangle$ and enter var$G$ in the leading order of perturbation.

III. CONDITIONS FOR PERTURBATIVE APPROACH

Traditionally conductance fluctuations in a system with broad, spatially homogeneous contacts are considered[1–5] by means of the Kubo formula[26]. Alternative considerations based on the Landauer-Büttiker formula[27] are more convenient in the presence of tunnel barriers[28] or for a lead geometry which involves spatially inhomogeneous currents. In this paper we will use this formula in the form first derived by Fisher and Lee:[29]

$$G = \frac{e^2}{2h} \sum_{ab} \left(T_{ab}^L + T_{ab}^R \right), \tag{6}$$

where the transmission coefficient $T_{ab}^{L(R)}$ is the probability of transmission from the channel labeled by a in the left (right) lead to the channel labeled by b in the right (left) lead. In the case of single-channel leads (of width $w \simeq \hbar k_F^{-1}$) the point-to-point conductance, G, is given by Eq. (6) without the summation sign, the transmission coefficients in this equation being related to Green's functions by[29]

$$T^{L(R)} = \frac{\alpha_1 \alpha_2}{(h\nu_0)^2} \left[\mathcal{G}^{+(-)}\left(\mathbf{r_1}, \mathbf{r_2}; \varepsilon\right) \mathcal{G}^{-(+)}(\mathbf{r_2}, \mathbf{r_1}; \varepsilon) \right], \tag{7}$$

where $\mathcal{G}^+$ ($\mathcal{G}^-$) is a retarded (advanced) Green's function, $\mathbf{r_1}$, $\mathbf{r_2}$ are the positions of the point contacts, and $\alpha_1\alpha_2$ is the transmission probability through the contacts themselves. In the entire energy interval of interest the mean density of states ν_0 is a constant and the $T^{L(R)}$ are energy independent so we will subsequently drop the ε label. Thus we imply that energy dependence will also be irrelevant for the conductance fluctuations: as usual, this is valid when the energy difference between two conductances, ω, is much smaller than the level broadening which we assume to be the case.

We consider the region of parameters defined by

$$\Delta \lesssim \gamma_{\rm esc} \ll \min\left\{\hbar/\tau_\phi\,,\,T\,,\,\hbar/\tau_{\rm erg}\right\}\,, \qquad (8)$$

Here the level broadening due to escape from the dot is represented by $\gamma_{\rm esc} \approx \Delta(\alpha_1+\alpha_2)+\gamma_{\rm leak}$ where $\gamma_{\rm leak}$ is the level broadening due to escape from the dot other than through the point contacts, for example due to leakage through the dot matrix.

Our perturbative approach is formally applicable both to the non-ergodic diffusive regime, $\tau_\phi \lesssim \tau_{\rm erg}$, and to the ergodic zero-mode regime, $\tau_\phi \gtrsim \tau_{\rm erg}$. The inequality $\gamma_{\rm esc} \ll \min(\hbar/\tau_\phi, T)$ is a crucial distinction from the imaginary potential model[7,9,15] where the opposite inequality holds. This allows us to separate dephasing processes inside the dot from those due to weak particle leakage. The latter have been introduced only for convergence of the perturbative approach which is not valid for $\gamma_{\rm esc} < \Delta$. Therefore, a weak violation of particle conservation is inevitable in the perturbative approach as will be explicitly shown later. However, this weak particle non-conservation is not related to the level broadening due to dephasing inside the dot and, as we shall see, may be totally neglected in the final results. On the contrary, in the imaginary potential model both the level broadening and the particle non-conservation have exactly the same source and cannot be separated which makes this model unsuitable for considerations of the influence of inelastic processes inside the dot on the conductance distribution.

The nonperturbative region $\gamma_{\rm esc} < \Delta$ was the main area of interest for previous zero mode calculations.[6,9,7] However, the exact zero-mode calculations within the nonlinear σ model cannot be extended (at least, in a straightforward way) to include relaxation processes inside the dot by simply introducing τ_ϕ. The reason is that all intra-sample diffusons *must* and all intrinsic diffusons *must not* contain a cutoff proportional to τ_ϕ^{-1}. These two kinds of diffusons which are both elementary excitations in the nonlinear σ model must be distinguished automatically. This can be easily done in the perturbative approach to the σ model[5] by the introduction of an extra set of matrix indices to numerate different conductance loops. While this additional dependence does not lead to any complication in perturbative or renormalization group calculations, it would make direct zero mode calculations rather difficult if possible at all. Obviously, one circumvents this complication when dephasing is included phenomenologically, as in the voltage probe model where one can proceed with zero-mode calculations.[17,18] However, there is a price to pay: as two kinds of diffusons are not distinguished, this model contains τ_ϕ proportional corrections to the mean conductance[18] even in the absence of time-reverse invariance when such corrections cannot appear in all orders of perturbation as we will show below.

The present model overlaps with the voltage probe model in the ergodic zero-mode regime (with strong dephasing): $\tau_{\rm erg} \ll \tau_\phi \ll \tau_{\rm esc}$. Even in this case, the overlapping is restricted to the region $\gamma_{\rm esc} \gtrsim \Delta$ as the requirement of convergence of perturbation series does not allow us to take the limit $\gamma_{\rm leak} \to 0$. Nevertheless, both the models address clearly the same physical situation where dephasing occurs inside the dot, and the results of the present considerations are in a broad agreement with the voltage probe model. Moreover, we shall argue later that the perturbative approach might be valid even outside the formal limits of applicability. Note finally that since our considerations always refer to strong dephasing with a noticeable leakage ($\gamma_{\rm leak} \gtrsim \Delta$), the results are applicable both for statistics of the heights of the Coulomb blockade peaks (for $\alpha_{1,2} \ll 1$) and for the conductance distribution of a single-channel cavity (for $\alpha_{1,2} \lesssim 1$).

Conductance cumulants $\langle\langle G^n \rangle\rangle$ are given by

$$\langle\langle G^n \rangle\rangle = \left(e^2/h\right)^n \left\langle\left\langle \left(T^L + T^R\right)^n \right\rangle\right\rangle, \qquad (9)$$

where $T^{(L,R)}$ should be expressed in terms of Green's functions, Eq. (7), and an extra prefactor of 2 is due to spin. Fisher and Lee[29] have shown that the unitarity of the S matrix implies $T^R = T^L$ even in the absence of time reversal invariance (in[30] the proof of this equality for a two lead system has been explicitly based on particle conservation). In the imaginary potential model of Refs. 7,9,15 the particle number is not conserved and, if time reversal symmetry is broken, $T^R \neq T^L$ as we will show explicitly later. That is why the conductance distribution in the absence of time reversal symmetry obtained[15] from the microscopic formula (6) turns out to be different from that obtained[9,7] from the reduced formula $G = (e^2/h)T^L$.

IV. MEAN CONDUCTANCE

In the model under consideration, the particle number is *almost* conserved: for the sake of convergence we have introduced $\gamma_{\rm esc} \gtrsim \Delta$ which describes particle leakage; however, in the region of interest, $\gamma_{\rm esc} \ll \hbar/\tau_\phi$, the leakage effect is small and we will show that in the leading order approximation $T^R = T^L$. On average though, $\langle T^R \rangle = \langle T^L \rangle$ so that the calculation of the mean conductance is straightforward.

The mean conductance $\langle G \rangle$ is clearly proportional to the Fourier transform at zero frequency of the density-density correlation function, Eq. (5). For the parametric region of Eq. (8) and for point contacts separated by a large distance, $R \equiv |\mathbf{r_1} - \mathbf{r_2}| \gg \ell$, $\langle G \rangle$ is dominated by the one-diffuson contribution shown in Fig. 2.

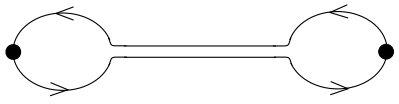

FIG. 2. The diagram for the mean conductance.

Obviously, this is the *intrinsic* diffuson, obeying particle conservation. At each end of the diffuson there are two-sided 'petal' shapes given analytically by

$$\chi_2(\mathbf{r},\mathbf{r}') = \left\langle \mathcal{G}^+(\mathbf{r}-\mathbf{r}')\right\rangle \left\langle \mathcal{G}^-(\mathbf{r}'-\mathbf{r})\right\rangle \tag{10}$$

The filled circles at the petals correspond to the constants $\alpha_{1,2}/(2\pi\nu_0)$ where $\alpha_{1,2}$ are the transmission probabilities through the contacts (here and elsewhere we put $\hbar$ to 1 in all intermediate expressions). The petals correspond to motion at ballistic scales since the average Green's functions $\langle \mathcal{G}^{\pm}(\mathbf{r},\mathbf{r}')\rangle$ (drawn as edges of the petal) decay like $\exp(-|\mathbf{r}-\mathbf{r}'|/2\ell)$. At the diffusive scale, $|\mathbf{r}-\mathbf{r}'| \gtrsim \ell$, the petals may be approximated by $\chi_2(\mathbf{r},\mathbf{r}') = \chi_2\,\delta(\mathbf{r}-\mathbf{r}')$ where the constant χ_2 is given by[31]

$$\chi_2 = \int \left\langle \mathcal{G}^+(\mathbf{r}-\mathbf{r}')\right\rangle \left\langle \mathcal{G}^-(\mathbf{r}'-\mathbf{r})\right\rangle \mathrm{d}^d r = \int \left\langle \mathcal{G}^+(\mathbf{p})\right\rangle \left\langle \mathcal{G}^-(\mathbf{p})\right\rangle \mathrm{d}^d p = \nu_0 \int_{-\varepsilon_F}^{\infty} \frac{\mathrm{d}\xi}{\xi^2+\frac{1}{4\tau^2}} \approx 2\pi\nu_0\tau\,. \tag{11}$$

where $\xi = p^2/2m - \varepsilon_F$. Then one finds

$$\langle G\rangle = 2A\int \chi_2(\mathbf{r_1},\mathbf{r_1'})\mathcal{D}(\mathbf{r_1'},\mathbf{r_2'};\gamma_{\rm esc})\chi_2(\mathbf{r_2},\mathbf{r_2'})\,\mathrm{d}^d r_1'\mathrm{d}^d r_2' = \frac{e^2}{2\pi}\alpha_1\alpha_2\zeta_{\rm esc}(R)\,,\quad A \equiv \frac{e^2}{2\pi}\frac{\alpha_1\alpha_2}{(2\pi\nu_0)^2}\,, \tag{12}$$

where $R \equiv |\mathbf{r}_1-\mathbf{r}_2|$, and $\zeta_{\rm esc}(R)$ is defined by

$$\zeta(R) \equiv 2\tau^2\mathcal{D}(\mathbf{r}_1,\mathbf{r}_2;i\gamma) = \frac{\Delta}{\pi}\sum_{\mathbf{q}}\frac{e^{i\mathbf{q}\cdot(\mathbf{r}_1-\mathbf{r}_2)}}{D\boldsymbol{q}^2+\gamma}\,, \tag{13}$$

with $\gamma = \gamma_{\rm esc}$. As $\gamma_{\rm esc} \ll E_c$ in the parametric regime (8), $\zeta_{\rm esc}(R)$ is dominated by the zero-mode contribution ($q=0$) only. Therefore,

$$\zeta_{\rm esc}(R) \approx \frac{\Delta}{\pi\gamma_{\rm esc}}\,. \tag{14}$$

Combining Eqs. (12) and (14), one finds

$$\langle G\rangle = \frac{e^2}{\pi h}\frac{\alpha_1\alpha_2\Delta}{\gamma_{\rm esc}}\,. \tag{15}$$

As expected in the zero-mode approximation, $\langle G\rangle$ is independent of the separation of the point contacts, the dimensionality, and the degree of disorder. The perturbation expansion for $\langle G\rangle$ is strictly valid only in the regime where $\zeta_{\rm esc} \ll 1$. Without introducing $\gamma_{\rm leak}$, we would have $\gamma_{\rm esc} \approx \Delta(\alpha_1+\alpha_2) \ll \Delta$ so that $\zeta_{\rm esc} \gg 1$. However, substituting this value of $\zeta_{\rm esc}$ into Eq. (12) reproduces the result of the voltage probe model for the classical mean conductance[18] which corresponds to the standard single-channel conductance.

This means that all perturbative corrections to $\langle G\rangle$ either vanish or cancel each other. In the absence of time reversal symmetry, higher order corrections could result from the expansion in the diffuson loops only. In the usual case of broad contacts, one should sum over all q in Eq. (13) which leads to the parameter, $g_0^{-1}\ln L/\ell$ at $d=2$. It is well known that all the 'main logarithms', $g^{-n}\ln^n\omega\tau$, are mutually cancelled due to the renormalizability in all orders of perturbation.[22,32,14] The first nonvanishing contribution arises in the second order and is proportional to $g^{-2}\ln\omega\tau$ in correspondence with the renormalization group results.[32,14] However, in the zero mode regime considered here there is complete cancellation at least up to the fourth order similar to that occurring in the same regime in calculating the energy-level correlation function[33]. This is easy to verify as the calculation is much simpler than the standard one in the diffusive regime. One could assume that the cancellation of the main logarithms in all higher orders in the diffusive regime corresponds to a similar cancellation of the zero mode contributions. Since in the latter case there is no renormalization group backing, such a cancellation remains only a plausible hypothesis. Nevertheless, it is certain that in the absence of time-reversal invariance no correction due to dephasing may appear as they are forbidden by particle conservation. When time-reversal symmetry is not broken, there exist weak localization (Cooperon) corrections in the lowest order which are proportional to the standard $g^{-1}\ln\tau_\phi/\tau$ in the non-ergodic diffusive regime, $\tau_\phi \ll \tau_{\rm erg}$, or to Δ/τ_ϕ in the ergodic zero-mode regime, $\tau_\phi \gg \tau_{\rm erg}$. In any case, in the region of Eq. (8) these corrections are negligible, and the main result is given by Eq. (15).

V. VARIANCE OF CONDUCTANCE

The lowest order diagrammatic contribution to the variance is given in Fig. 3, for clarity both in the standard representation [1–4] and in that with diffusion modes separated from ballistic ones[22] as in Fig. 1. Although the diagram in Fig. 3a looks precisely like one of the leading diagrams[1–5] for the UCF, the result of the calculation is absolutely different due to the fact that the vertices of both conductance loops correspond to the point contacts. This is most clear in the representation of Fig. 3b where local petals are connected together by two inter-sample diffusons. The petals reduce to the same constant as for the mean conductance, Eq. (11). Thus, one finds by analogy with Eq. (12) that this diagram's contribution to the variance is

$$2A^2\chi_2^2\mathcal{D}^2(\boldsymbol{r}_1,\boldsymbol{r}_2;\,i\gamma_\phi)\,,$$

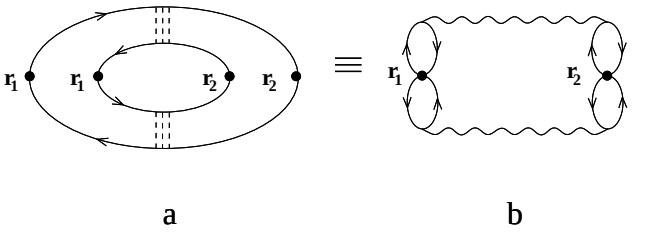

FIG. 3. The lowest-order contributions to the variance. Wavy lines represent diffuson ladders which correspond to the inter-sample diffusons. The relation between a wavy line and a ladder is the same as for intrinsic diffusons, Fig. 1.

where the constant A is the overall factor in the expression for $T^{L,R}$ in terms of Green's function, Eq. (7), this factor being explicitly defined in Eq. (12). Substituting the values of all constants and taking into account the contribution of the equivalent Cooperon diagram (obtained from that in Fig. 3a by inverting the direction of arrows in one of the loops) results in the following expression

$$\left\langle\!\left\langle G^2 \right\rangle\!\right\rangle^{(1)} = \frac{1}{\beta}\left[\frac{e^2}{h}\alpha_1\alpha_2\,\zeta_\phi(R)\right]^2 . \qquad (16)$$

Here $\zeta_\phi(R)$ is given by Eq. (13) with $\gamma = \tau_\phi^{-1}$. Its value depends on whether one considers the non-ergodic diffusive regime, $\tau_\phi \ll \tau_{\rm erg}$, or the ergodic zero-mode regime, $\tau_\phi \gg \tau_{\rm erg}$. In the former case, the summation in Eq. (13) may be approximated by an integration with cutoff at $q \sim L_\phi^{-1} = (D\tau_\phi)^{-1/2}$, while in the latter case only the $q = 0$ term makes a relevant contribution to the sum. This leads to the expression for $\zeta_\phi(R)$ given in the Introduction, Eq. (2). The contribution (16) to the variance differs from $\langle G\rangle^2$ by the substitution of $\zeta_\phi(R)$ for $\zeta_{\rm esc}(R)$. As $\zeta_\phi(R) \ll \zeta_{\rm esc}(R)$ in the region (8), this difference (which is absent in the imaginary potential model[7,9,15]) is crucial for the description of dephasing within the dot.

It is important that the diffuson and Cooperon diagrams originate from different terms in Eq. (9). Indeed, a diffuson ladder connects $\mathcal{G}^+$ and $\mathcal{G}^-$ lines which have the opposite directions, while a Cooperon ladder connects $\mathcal{G}^+$ and $\mathcal{G}^-$ with the same direction. Therefore, in the diffuson diagram in Fig. 3a $\mathcal{G}^+$'s have the same direction in both loops. Then it follows from the expression for $T^{(L,R)}$ in terms of Green's functions, Eq. (7), that this diagram originates from $\left\langle \left(T^L\right)^2\right\rangle + \left\langle \left(T^R\right)^2\right\rangle$. As the direction of arrows must be inverted in one of the loops in order to obtain an equivalent Cooperon diagram, in this diagram $\mathcal{G}^+$'s have the opposite directions so that it originates from $2\left\langle T^L\,T^R\right\rangle$. Considering

$$\left\langle \left(T^L - T^R\right)^2\right\rangle = 2\left\langle \left(T^L\right)^2\right\rangle - 2\left\langle T^L\,T^R\right\rangle , \qquad (17)$$

where, in this lowest diagrammatic order, the first contribution is given by the diffuson diagram while the second is given by the Cooperon diagram, one can see that $T^L \neq T^R$ for $\beta = 2$ (in the absence of time reversal symmetry) when the Cooperon contribution vanishes. For $\beta = 1$ the two contributions in Eq. (17) cancel each other. In the imaginary potential model[7,9,15] the lowest order diagrams make the leading contributions to the variance. Therefore, in this case the reduced formula $G \propto T^L$ is not equivalent to the microscopically derived[29] formula (6). Since the $T^L = T^R$ equality is based on particle conservation, its breakdown in the imaginary potential model is another clear indication of the absence of particle conservation.

In the present model where the particle number is 'almost' conserved, the breakdown of this equality in the lowest order indicates that the higher order diagrams must be more relevant. This is indeed the case since the condition $\zeta_\phi \ll \zeta_{\rm esc}$ suggests that the dominant contribution to the variance in the region (8) is given by diagrams which contain the lowest possible number of intrinsic diffusons ($\zeta_{\rm esc}$) and have their conductance loops connected *by only one* inter-sample diffuson (ζ_ϕ).

Two such diagrams are shown in Fig. 4 in the two equivalent representations described above. Directions of arrows are chosen in such a way that all propagators in both the diagrams are diffusons. Inverting the direction of arrows in one of the conductance loops in diagrams (a) and (c), one converts inter-sample diffusons into Cooperons, leaving intrinsic diffusons intact. In the diffuson diagram (4a), $\mathcal{G}^+$'s have opposite directions in different conductance loops so that it originates from $2\left\langle T^L\,T^R\right\rangle$. On the contrary, $\mathcal{G}^+$'s have the same directions in both loops in the diagram (4c) so that this diagram originates from $\left\langle \left(T^L\right)^2\right\rangle + \left\langle \left(T^R\right)^2\right\rangle$. Thus, in contrast to the lowest order diagrams in Fig. 3, even for $\beta = 2$ when time-reversal symmetry is broken, both $2\left\langle T^L\,T^R\right\rangle$ and $\left\langle \left(T^L\right)^2\right\rangle + \left\langle \left(T^R\right)^2\right\rangle$ contribute to the conductance.

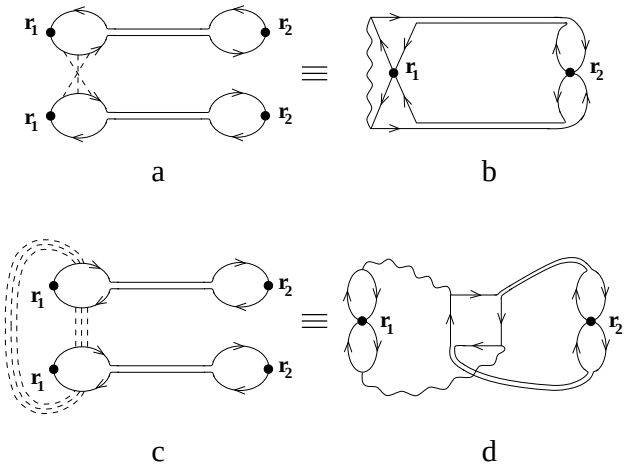

FIG. 4. The leading diagrammatic contribution to the variance. In the diagrams *b* and *d*, the inter-sample diffusons are represented by wavy lines and the intrinsic diffusons by double lines.

The calculation of these diagrams is described in the Appendix. For simplicity, we did not draw single-impurity lines in diagrams in Fig. 4c and 4d which "dress" in a standard way[22] the inner square in Fig. 4d. Such a dressing results in an exact cancellation of one of the inter-sample diffusons (wavy lines) by the square which makes the contribution of the diagram 4d equal to that of the diagram 4b. In addition to these diagrams, one can construct only one more contribution to the variance which contains two diffuson loops. This contribution describes a weak-localization correction to a diffuson and contains three intra-sample ladders thus being small even compared to the contribution of Eq. (16).

Adding together the contributions of all relevant diffuson and Cooperon diagrams in this order, we find

$$\left\langle\!\left\langle G^2 \right\rangle\!\right\rangle^{(2)} = \frac{4}{\beta}\left[\frac{e^2\alpha^2}{h}\zeta_{\rm esc}(R)\right]^2 \zeta_\phi(\ell)\,. \tag{18}$$

Comparing Eqs. (18) and (16), one has

$$\frac{\left\langle\!\left\langle G^2 \right\rangle\!\right\rangle^{(2)}}{\left\langle\!\left\langle G^2 \right\rangle\!\right\rangle^{(1)}} \gtrsim \frac{\zeta_{\rm esc}^2}{\zeta_\phi(\ell)} \gg 1 \tag{19}$$

in the parametric region (8) corresponding to strong dephasing since $\zeta_\phi(\ell)$ is small while $\zeta_{\rm esc}$ is close to 1. Therefore, in this regime the variance is dominated by the non-universal contribution of Eq. (18). Substituting the expression for $\langle G\rangle$ into Eq. (18), we obtain the result of Eq. (1) given in the Introduction.

Let us stress that the exact equality of the diffuson diagrams (4a) originating from $\left\langle T^L\,T^R\right\rangle$ and (4c) originating from $\left\langle \left(T^R\right)^2\right\rangle$ ensures that the two terms in Eq. (17) cancel each other even in the case $\beta = 2$ when there are no Cooperon contributions. The same is valid for the leading contribution to the higher order moments of $T^L - T^R$. Therefore, keeping only the leading contribution and neglecting sub-dominant contributions to $\left\langle\!\left\langle G^n \right\rangle\!\right\rangle / \langle G\rangle^n$ which are due to a small particle leakage, one finds that $T^L = T^R$ as expected in any particle conserving model.

VI. HIGHER MOMENTS AND DISTRIBUTION OF CONDUCTANCE

In order to determine the distribution, we need to find the leading contributions to the nth cumulant. The lowest order diagrams are a generalisation of those for the variance[15], Fig. 3. They have two n-petal daisy vertices, the petals being connected by n inter-sample diffusion propagators. Each diagram gives a contribution of $(n-1)!\,\langle G\rangle^n\,[\zeta_\phi(R)/\zeta_{\rm esc}(R)]^n$ where a factor of $(n-1)!$ arises upon counting all possible ways of ordering the n loops. Diagrams which generalize the leading order contribution to the variance for $n = 3$ are shown in Fig. 5.

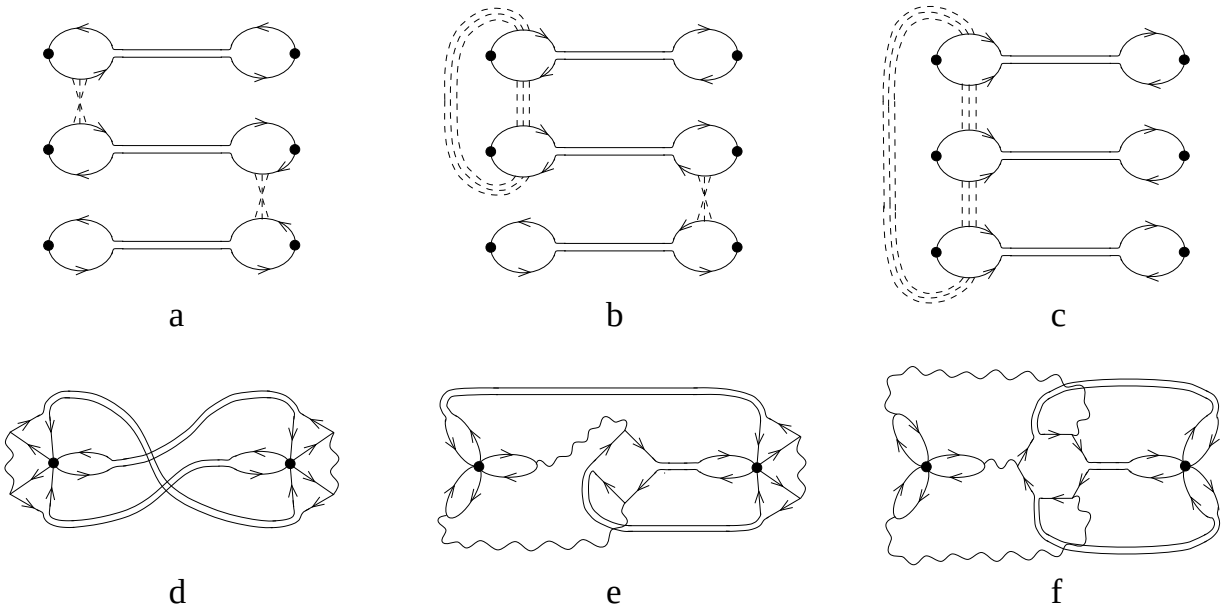

FIG. 5. Some of the diagrams making a leading contribution to the third moment of conductance. Diagrams in the second row are equivalent to their counterparts in the first row.

In general, such diagrams are obtained by taking n conductance loops, each loop having an intra-sample diffuson (as for the mean, Fig. 2), and connecting these loops with the least possible number of inter-sample diffusons. Actually, the number of inter-sample diffusons may vary, as every inner polygon (like the inner square in diagram $4d$ for the variance) cancels one of them (see Appendix). It is the number of loops consisting of inter-sample diffusons which should be minimal.

For the third cumulant (Fig. 5.), each diagram has two such loops. The lowest order diagram, two three-petal daisies connected by three inter-sample diffusons, also has two diffuson loops. However, there is no cancellation there and this diagram is proportional to $\zeta_\phi(R)^3$. Each diagram in Fig. 5 is proportional to $\zeta_\phi^2(\ell)\zeta_{\rm esc}^3$. As we are interested in the case of strong dephasing ($\zeta_\phi \ll 1$) and weak leakage $\zeta_{\rm esc} \sim 1$, this contribution is dominant. Note that Fig. 5 does not include all the diagrams of this order, and a numerical factor attached to the leading contribution to $\langle\langle G^n \rangle\rangle$ is not easy to calculate for $n = 3$ and hardly possible for arbitrary n. However, this is not necessary for what follows. It is sufficient to know that the leading contribution to the nth cumulant is proportional to $\zeta_\phi^{n-1}(\ell)\,\zeta_{\rm esc}^n$. Thus, keeping both the lowest order and the leading contribution, we find

$$\frac{\langle\langle G^n \rangle\rangle}{\langle G \rangle^n} = \frac{(n-1)!}{\beta}\left\{\left[\frac{\zeta_\phi(R)}{\zeta_{\rm esc}(R)}\right]^n + c_n\ \left[\zeta_\phi(\ell)\right]^{n-1}\right\}, \quad (20)$$

where n-dependence of c_n is much slower than factorial (although it might include a trivial factor like 2^n or so). For weak particle escape and strong dephasing, Eq. (8), the second term in Eq. (20) dominates. Comparison of this dominant contribution to an appropriate power of the variance gives

$$\frac{\langle\langle G^n \rangle\rangle^2}{(\mathrm{var}\, G)^n} \sim \left[\zeta_\phi(\ell)\right]^{n-2} \ll 1\,,$$

so that the distribution is mainly Gaussian with non-universal variance $\mathrm{var}\, G$ given by Eqs. (1) and (18). Note that this is similar to the behavior of the higher order cumulants[5] in the case of UCF in a sample with broad contacts, where such a ratio is proportional to $g_0^{-2(n-2)}$. Very high cumulants, with $n \gtrsim g_0^{-1}$, grow much faster which leads to lognormal tails of the distribution[15] similar to those[5] for samples with broad contacts. At weak disorder the lognormal tails are practically irrelevant as they start at $\delta G \sim \langle G \rangle \sqrt{g_0} \gg \langle G \rangle$ where $\delta G = G - \langle G \rangle$, while typical deviations $\delta G \sim \sqrt{\mathrm{var}\, G} \ll \langle G \rangle$.

In the presence of some particle leakage from the dot, $\zeta_{\rm esc}(R) \gtrsim 1$, the exponential tails are more important, these tails being governed by first term in Eq. (20) which dominates for larger n. It turns out that the exponential tails dominate the Gaussian ones for

$$(\delta G)^2 \gg \mathrm{var}\, G\, \frac{\zeta_{\rm esc}^2}{\zeta_\phi}\,. \quad (21)$$

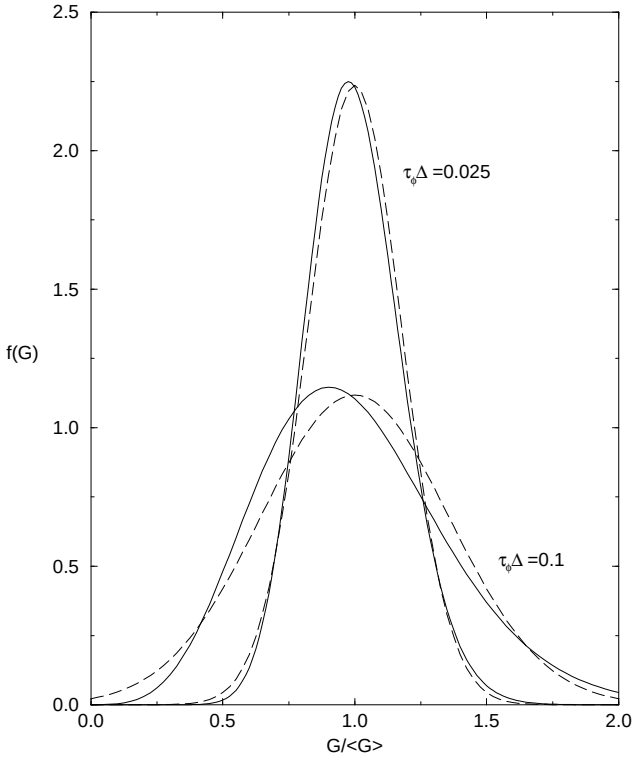

FIG. 6. Solid curves show the conductance distribution for $\beta = 1$ with dephasing rates $\Delta\tau_\phi = 0.1$ and 0.025, calculated using the second term in Eq. (20) with an arbitrarily chosen coefficient $c_n = 2^{n-1}n$. For comparison the dashed curves are Gaussian distributions with the same mean and variance.

This estimation results from a comparison of the exponential distribution obtained using the first term in Eq. (20) with the Gaussian distribution with the variance (18) obtained by neglecting the higher cumulants.

For weak particle leakage, the exponential tails start at deviations which are much stronger than typical ones. With increasing leakage, these tails become important at the same values of $\zeta_{\rm esc}$ at which the variance is mainly contributed by escape processes, Eq. (19). Inequalities (19) and (21) show that the crossover to the regime dominated by particle escape happens not at $\tau_{\rm esc} \sim \max(\tau_\phi, \tau_{\rm erg})$ but at considerably weaker particle escape: either at $\tau_{\rm esc} \sim \sqrt{\tau_\phi/\Delta} \gg \tau_\phi$ in the ergodic regime ($\tau_\phi \gg \tau_{\rm erg}$), or at $\tau_{\rm esc} \sim \sqrt{\tau_{\rm erg}/\Delta} \gg \tau_{\rm erg}$ in the diffusive regime ($\tau_\phi \ll \tau_{\rm erg}$). Note that in Eqs. (19) and (21) we have disregarded the difference between $\zeta_\phi(R)$ and $\zeta_\phi(\ell)$ which is exact in the zero-mode regime and logarithmically accurate in the diffusive regime at $d = 2$. In the diffusive regime at $d = 3$, this difference is significant as may be seen from Eq. (2). Taking this into account will introduce an extra small factor of ℓ/R into the r.h.s. of the estimations (19) and (21) thus suppressing a relative importance of escape processes.

In the case of main interest, when particle leakage may be neglected, the distribution still deviates from Gaussian since the cumulants, given by the second term in Eq. (20), do not vanish although they are small. The distribution can be restored from these cumulants in a standard way (see, e.g., Ref. 5). Exact values of the coefficient c_n do not matter as the most relevant contribution to the deviation from a Gaussian shape is given by the third cumulant, similarly to the case of the conductance fluctuations in samples with broad leads.[34] The resulting distributions are shown for two values of $\tau_\phi/\tau_{\rm erg}$ in Fig. 6. It is seen that deviations from the Gaussian shape are not very strong.

In conclusion, we have found that the conductance distribution for disordered quantum dots with single-channel leads becomes mainly Gaussian for strong dephasing, $\tau_\phi \ll h/\Delta$, in broad agreement with the voltage probe model of Ref. 18. Let us stress again that since we have assumed non-zero $\gamma_{\rm leak}$ in this paper, there is no exact region of overlap between our results and those of the voltage probe model. Therefore, a direct comparison of the results is not possible. However there remain some noticeable differences, first of all in the dependence of the variance of the Gaussian distribution on τ_ϕ. If we stretch our results to the limit of applicability putting $\zeta_{\rm esc} = 1$ and making the contacts transparent ($\alpha_1 = \alpha_2 = 1$), we will have ${\rm var}G \sim \tau_\phi$ while the result of Ref. 18 for transparent contacts is ${\rm var}G \sim \tau_\phi^2$. Note that although in our approach resummation in all powers of $\zeta_{\rm esc}$ might be necessary for $\zeta_{\rm esc} \lesssim 1$, it could not change the dependence of the result on τ_ϕ. Similarly, in contrast to another result of Ref. 18, the dephasing rate τ_ϕ^{-1} could not appear in the mean conductance in the unitary case, $\beta = 2$. Indeed, in this case Cooperons vanish, and particle conservation strictly prohibits the appearance of τ_ϕ^{-1} in any power of expansion in diffusons. However, this disagreement is minor, and is clearly due to differences between the models. Let us stress that in contrast to the imaginary potential model, our present microscopic considerations confirm the prediction of the voltage probe model on the Gaussian character of the conductance distribution with a non-universal variance depending on the dephasing rate.

The most distinctive feature of the perturbative approach used here was taking into account two different sources of level broadening, one due to the presence of contacts entering the classical part of the mean conductance, and the other due to dephasing, appearing only in weak localization corrections and fluctuations. It remains an open question as to whether a similar introduction of two different sources of level broadening could be used within a non-perturbative approach such as the supersymmetric nonlinear σ model, thus enabling a calculation for $\gamma_{\rm leak} = 0$.

ACKNOWLEDGMENTS

We are grateful to C. W. J. Beenakker, M. Leadbeater, and R. A. Smith for useful discussions. Work in Birmingham has been supported by EPSRC grants GR/J35238 and GR/K95505.

APPENDIX A: CALCULATION OF THE LEADING CONTRIBUTION TO THE VARIANCE

The calculation of the diagrams in Fig. 4 is straightforward in the representation (*b*) and (*d*). The contribution of diagram (*b*) is given by

$$8A^2|\chi_3|^2\chi_2^2\mathcal{D}(\boldsymbol{r}_1,\boldsymbol{r}_1;\,i\gamma_\phi)\mathcal{D}^2(\boldsymbol{r}_1,\boldsymbol{r}_2;\,i\gamma_{\rm esc})\,. \qquad \text{(A1)}$$

Here the overall factor of 8 takes into account that diagram (4*b*) originates from $\langle T^L T^R\rangle$, and there are four ways to connect T^R and T^L with an inter-sample diffuson which is clear from the equivalent representation of this diagram, Fig. 4*a*. The constant χ_3 is contributed by a triangle consisting of three Green's functions. This is a constant since, similarly to the calculation of the mean conductance, Eq. (12), the triangle may be approximated at the diffusive scale, $|\mathbf{r}-\mathbf{r}'| \gtrsim \ell$, by $\chi_3(\mathbf{r},\mathbf{r}',\mathbf{r}'') = \chi_3\,\delta(\mathbf{r}-\mathbf{r}')\,\delta(\mathbf{r}-\mathbf{r}'')$. The presence of the δ functions ensures that the contribution of this diagram, Eq. (A1), reduces to a mere product of the local contributions, χ_2 and χ_3, and the diffusons, where the constant χ_3 is given by

$$\chi_3 = \int \left\langle \mathcal{G}^+(\mathbf{p})\right\rangle^2 \left\langle \mathcal{G}^-(\mathbf{p})\right\rangle {\rm d}^d p = -2\pi i\nu_0\tau^2\,. \qquad \text{(A2)}$$

At the same scale, the spatial arguments in $\mathcal{D}(\boldsymbol{r}_1,\boldsymbol{r}_1;\,i\gamma_\phi)$ coincide within an accuracy of order ℓ. Therefore, $2\tau^2\mathcal{D}(\boldsymbol{r}_1,\boldsymbol{r}_1;\,i\gamma_\phi) = \zeta_\phi(R=\ell) \equiv \zeta_\phi(\ell)$ by the definition of Eq. (13) with $\zeta_\phi(R)$ given by Eq. (2). Substituting all the constants into Eq. (A1), we obtain the contribution of diagram (*b*) as follows

$$\left[\frac{e^2\alpha_1\alpha_2}{h}\zeta_{\rm esc}(R)\right]^2 \zeta_\phi(\ell) = \zeta_\phi(\ell)\,\left\langle G\right\rangle^2\,. \qquad \text{(A3)}$$

The contribution of diagram (4*d*) is given by

$$4A^2\chi_2^4\mathcal{D}^2(i\gamma_{\rm esc})\int \hat{\chi}_4(\boldsymbol{r})\,\mathcal{D}^2(\boldsymbol{r_1},\boldsymbol{r};i\gamma_\phi){\rm d}^d r\,. \qquad \text{(A4)}$$

Here χ_4 is contributed by the "dressed" inner square which is the sum of one "bare" square and two squares containing one single-impurity line each, this line connecting opposite sides of the square.[22] The factor of 4 arises because diagram (4*d*) originates from $\left\langle \left(T^L\right)^2\right\rangle + \left\langle \left(T^R\right)^2\right\rangle$ and there are only two ways to connect the conductance loops with two inter-sample diffusons which is clear from the equivalent representation, Fig. 4*c*.

The calculation is more transparent in the ergodic zero-mode regime, $\tau_{\rm erg} \ll \tau_\phi \ll \hbar/\Delta$, when not only the intrinsic diffuson, Eq. (2), but also the inter-sample diffuson, Eq. (14), and the dressed square, χ_4, reduce to a constant. Since the contribution of a single-impurity line is given by the correlator (3), one finds χ_4 as follows

$$\chi_4 = \int \left\langle \mathcal{G}^+ \right\rangle^2 \left\langle \mathcal{G}^- \right\rangle^2 \mathrm{d}^d p + \frac{1}{2\pi\nu_0\tau_{\rm el}} \left(\int \left\langle \mathcal{G}^+ \right\rangle^2 \left\langle \mathcal{G}^- \right\rangle \mathrm{d}^d p \right)^2$$

The first term is calculated in a similar manner to that in Eq. (11) which gives $4\pi\nu_0\tau^3$. The integral in the second term coincides with that in Eq. (A2) so that one obtains

$$\chi_4 = 4\pi\nu_0\tau^4 \left(\frac{1}{\tau} - \frac{1}{\tau_{\rm el}} \right) = \frac{4\pi\nu_0\tau^4}{\tau_\phi} \,. \qquad \text{(A5)}$$

The difference between the one-particle relaxation time, τ, and the mean elastic scattering time, $\tau_{\rm el}$, is crucial in this calculation; the same difference is a formal cause of the saturation of the inter-sample diffuson, Eq. (13), for $q = 0$ at $\gamma = 1/\tau_\phi$.

On substituting the zero-mode values of χ_4, Eq. (A5), and $\mathcal{D}(i\gamma_\phi)$, one reduces the integral in Eq. (A4) to

$$\int \hat{\chi}_4(\boldsymbol{r})\, \mathcal{D}^2(\boldsymbol{r_1}, \boldsymbol{r}; i\gamma_\phi) \mathrm{d}^d r = \frac{4\pi\nu_0\tau^4}{\tau_\phi} \frac{L^d \zeta_\phi^2}{(2\tau^2)^2} = \zeta_\phi \,, \quad \text{(A6)}$$

so that the dressed square, χ_4, exactly cancels one of the inter-sample diffusons. Then, on substituting Eq. (A6) and all the constants into Eq. (A4), one finds that in the zero-mode case (when $\zeta_\phi(\ell) \equiv \zeta_\phi = \Delta\tau_\phi/\pi$), this contribution equals that of diagram (4*b*), Eq. (A3). In Eq. (A5) we have neglected the $1/\tau_{\rm esc}$ contribution to the one-particle relaxation time, $1/\tau$. Taken into account, this would lead to an additional contribution of diagram (*d*) proportional to $\zeta_\phi^2\zeta_{\rm esc}$ rather than $\zeta_\phi\zeta_{\rm esc}^2$ as in Eq. (A3). In this contribution, the inner square cancels one of the intrinsic diffusons. Overall, such a contribution of diagram (*d*) would be exactly equal to the contribution of the diagram similar to that in Fig. (4*b*) but made from one intrinsic and two inter-sample diffusons. We neglect these contributions which are small even compared to those of the diagrams in Fig. (3).

We do not present here the calculation of $\hat{\chi}_4(\boldsymbol{r})$ in a general case, without the restriction to the zero-mode regime. The calculation is standard[22] and results in

$$\hat{\chi}_4(\boldsymbol{r}) = 2\pi\nu_0\tau^4 \Big(-D\nabla^2 + \gamma_\phi \Big) \,,$$

so that $\hat{\chi}_4(\boldsymbol{r})$ is proportional to the diffusion operator. Then using the diffusion equation one finds that

$$\int \hat{\chi}_4(\boldsymbol{r})\, \mathcal{D}^2(\boldsymbol{r_1}, \boldsymbol{r}; i\gamma_\phi) \mathrm{d}^d r = 2\tau^2 \mathcal{D}(\boldsymbol{r_1}, \boldsymbol{r}_1; i\gamma_\phi) = \zeta_\phi(\ell) \,,$$

which generalizes Eq. (A6) and shows that the contribution of diagram (4*d*) in this case is also exactly equal to that of diagram (4*b*), Eq. (A3).

Finally, the overall coefficient for the contribution of all the leading diagrams equals $4/\beta$, since in the orthogonal case ($\beta = 1$) an equal contribution is made by two equivalent Cooperon diagrams. This leads to the result of Eq. (18).

[1] B. L. Altshuler, Pis'ma v ZhETF **41**, 530 (1985) [JETP Letters **41**, 648 (1985)].

[2] P. A. Lee and A. D. Stone, Phys. Rev. Lett. **55**, 1622 (1985).

[3] B. L. Altshuler and D. E. Khmelnitskii, Pis'ma v ZhETF **42**, 291 (1985) [JETP Letters **42**, 359 (1985)].

[4] P. A. Lee, A. D. Stone, and H. Fukuyama, Phys. Rev. **B 35**, 1039 (1987).

[5] B. L. Altshuler, V. E. Kravtsov, and I. V. Lerner, Zh. Eksp. Teor. Fiz. **91**, 2276 (1986) [Sov. Phys. JETP **64**, 1352 (1986)].

[6] H. U. Baranger and P. A. Mello, Phys. Rev. Lett. **73**, 142 (1994). R. A. Jalabert, J. L. Pichard, and C. W. J. Beenakker, Europhys. Lett **27**, 255 (1994).

[7] K. B. Efetov, Phys. Rev. Lett. **74**, 2299 (1995).

[8] R. A. Jalabert, A. D. Stone, and Y. Alhassid, Phys. Rev. Lett. **68**, 3468 (1992).

[9] V. N. Prigodin, K. B. Efetov, and S. Iida, Phys. Rev. Lett. **71**, 1230 (1993); Phys. Rev. **B 51**, 17223 (1995).

[10] A. M. Chang, H. U. Baranger, L. N. Pfeiffer, K. W. West, and T. Y. Chang, Phys. Rev. Lett. **76**, 1695 (1996). J. A. Folk, S. R. Patel, S. F. Godijn, A. G. Huibers, S. M. Cronenwett, C. M. Marcus, K. Campman, and A. C. Gossard, Phys. Rev. Lett. **76**, 1699 (1996).

[11] A. Kamenev and Y. Gefen, Europhys. Lett. **29**, 413 (1995).

[12] M. L. Mehta, *Random matrices* (Academic Press, NY, 1991).

[13] C. W. J. Beenakker, Rev. Mod. Phys. **69**, 731 (1997).

[14] K. B. Efetov, Adv. Phys. **32**, 53 (1983).

[15] E. McCann and I. V. Lerner, J. Phys.–Condensed Matter **8**, 6719 (1996).

[16] M. Büttiker, Phys. Rev. **B 33**, 3020 (1986).

[17] H. U. Baranger and P. A. Mello, Phys. Rev. **B 51**, 4703 (1995); P. W. Brouwer and C. W. J. Beenakker, Phys. Rev. **B 51**, 7739 (1995).

[18] P. W. Brouwer and C. W. J. Beenakker, Phys. Rev. **B 55**, 4695 (1997).

[19] I. H. Chan, R. M. Clarke, C. M. Marcus, K. Campman, and A. C. Gossard, Phys. Rev. Lett. **74**, 3876 (1995).

[20] R. A. Serota, S. Feng, C. Kane, and P. A. Lee, Phys. Rev. **B 36**, 5031 (1987).

[21] A. A. Abrikosov, L. P. Gor'kov, and I. E. Dzyaloshinskii, *Methods of Quantum Field Theory in Statistical Physics* (Pergamon, Oxford, 1965).

[22] L. P. Gor'kov, A. I. Larkin, and D. E. Khmel'nitskii, Pis'ma v ZhETF **30**, 248 (1979) [JETP Letters **30**, 229 (1979)]; S. Hikami, Phys. Rev. **B 24**, 2671 (1981).

[23] C. Castellani, C. DiCastro, G. Kotliar, and P. A. Lee, Phys. Rev. Lett. **56**, 1179 (1986).

[24] A. Schmid, Z. Phys. **271**, 251 (1974); B. L. Altshuler, A. G. Aronov, and D. E. Khmelnitsky, J. Phys. C. **15**, 7367 (1982).
[25] U. Sivan, Y. Imry, A. G. Aronov, Europhys. Lett. **28**, 115 (1994).
[26] R. Kubo, J. Phys. Soc. Jap. **12**, 570 (1957).
[27] R. Landauer, Philos. Mag. **21**, 863 (1970); M. Büttiker, Phys. Rev. Lett. **57**, 1761 (1986).
[28] S. Iida, H. A. Weidenmüller, and J. Zuk, Ann. Phys. (USA) **200**, 219 (1990).
[29] D. S. Fisher and P. A. Lee, Phys. Rev. **B 23**, 6851 (1981).
[30] C. M. Marcus, R. M. Westervelt, P. F. Hopkins, and A. C. Gossard, Chaos **3**, 643 (1993).
[31] Average Green's functions $\left\langle \mathcal{G}^{\pm}(\xi)\right\rangle = (\xi \pm i/2\tau)^{-1}$ include $\tau^{-1} = \tau_{\rm el}^{-1} + \tau_{\phi}^{-1} \approx \tau_{\rm el}^{-1}$. In calculating petals or any boxes containing filled circles (i.e. representing electron motion at the ballistic scale near the leads), one can safely substitute $\tau_{\rm el}$ for τ. However, the difference between $\tau_{\rm el}$ and τ is crucial in calculating 'dressed' inner boxes without external vertices like the square in diagram 4*d*, see Appendix.
[32] L. Schäfer and F. Wegner, Z. Phys. **B 38**, 113 (1980).
[33] J. T. Chalker, I. V. Lerner, and R. A. Smith, J. Math. Phys. **37**, 5061 (1996).
[34] M. C. van Rossum, I. V. Lerner, B. L. Altshuler, and T. M. Nieuwenhuizen, Phys. Rev. **B 55**, 4710 (1997).